nanomaterials

MDPI

*Supplementary Materials*

# Composition-dependent cytotoxic and antibacterial activity of biopolymer-capped Ag/Au bimetallic nanoparticles against melanoma and multidrug-resistant pathogens

**Alfonso Nieto-Argüello [1], David Medina-Cruz [2], Yeremi S. Pérez-Ramírez [1], Sergio A. Pérez-García [3], Miguel. A. Velasco-Soto [1], Zeinab Jafari [1], Israel De Leon [1], María Ujué González [4], Yves Huttel [5], Lidia Martínez [5], Álvaro Mayoral [6,7,8], Thomas J. Webster [2], José M. García-Martín [4] and Jorge L. Cholula-Díaz [1,*]**

[1] School of Engineering and Sciences, Tecnologico de Monterrey, Eugenio Garza Sada 2501, Monterrey 64849, N.L., Mexico; alfonsonieto25@gmail.com (A.N.-A.); yeremi_said@hotmail.com (Y.S.P.-R.); miguel.velasco85@tec.mx (M.A.V.-S.); ZJafari@tec.mx (Z.J.); ideleon@tec.mx (I.D.L)
[2] Department of Chemical Engineering, Northeastern University, Boston, MA 02115, USA; davidmedina-crz@gmail.com (D.M.-C.); websterthomas02@gmail.com (T.J.W.)
[3] Centro de Investigación en Materiales Avanzados, S. C. (CIMAV), Unidad Monterrey, Alianza Norte 202, C.P. 66628, Apodaca, NL, Mexico; alfonso.perez@cimav.edu.mx
[4] Instituto de Micro y Nanotecnología, IMN-CNM, CSIC (CEI UAM+CSIC), Isaac Newton 8, Tres Cantos 28760, Spain; maria-ujue.gonzalez@csic.es (M.U.-G.); josemiguel.garcia.martin@csic.es (J.M.G.-M.)
[5] Instituto de Ciencia de Materiales de Madrid, ICMM-CSIC, Sor Juana Inés de la Cruz 3, Madrid 28049, Spain; huttel@icmm.csic.es (Y.H.); lidia.martinez@icmm.csic.es (L.M.)
[6] Instituto de Nanociencia y Materiales de Aragón (INMA), CSIC-Universidad de Zaragoza, Pedro Cerbuna, Zaragoza 50009, Spain; amayoral@unizar.es
[7] Laboratorio de Microscopías Avanzadas (LMA), Universidad de Zaragoza, Zaragoza 50018, Spain
[8] Center for High-Resolution Electron Microscopy (ChEM), School of Physical Science and Technology (SPST), ShanghaiTech University, 393 Middle Huaxia Road, Pudong, 201210, Shanghai, China
* Correspondence: jorgeluis.cholula@tec.mx

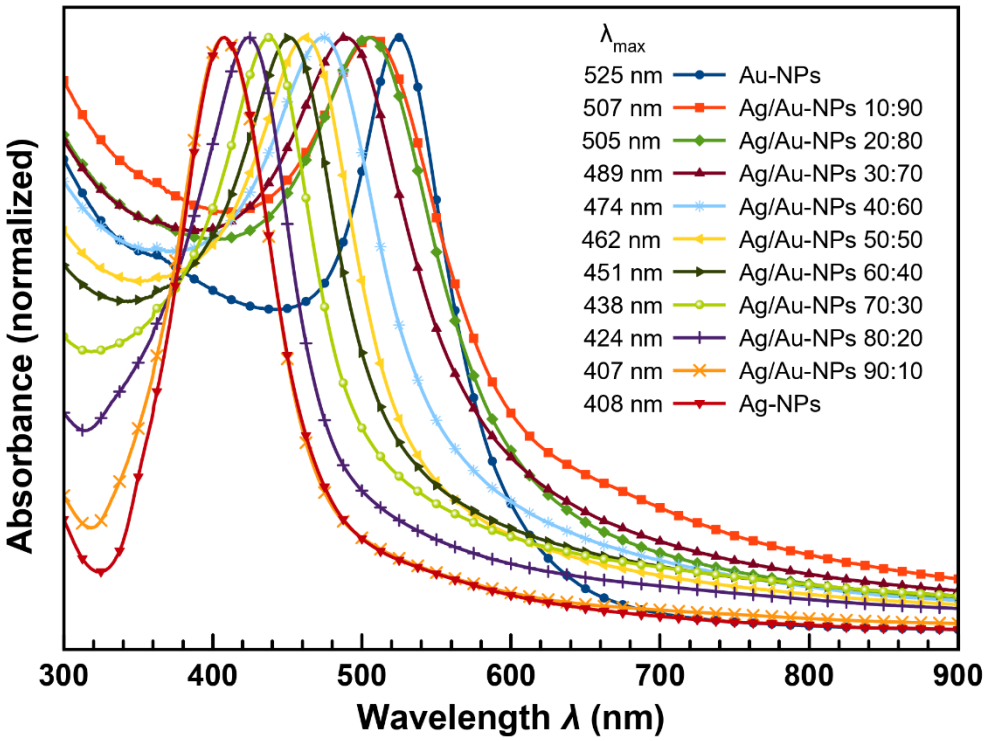


**Figure S1.** Normalized absorption spectra of colloidal Ag/Au-NPs in the complete atomic chemical composition range with steps of 10 at%.

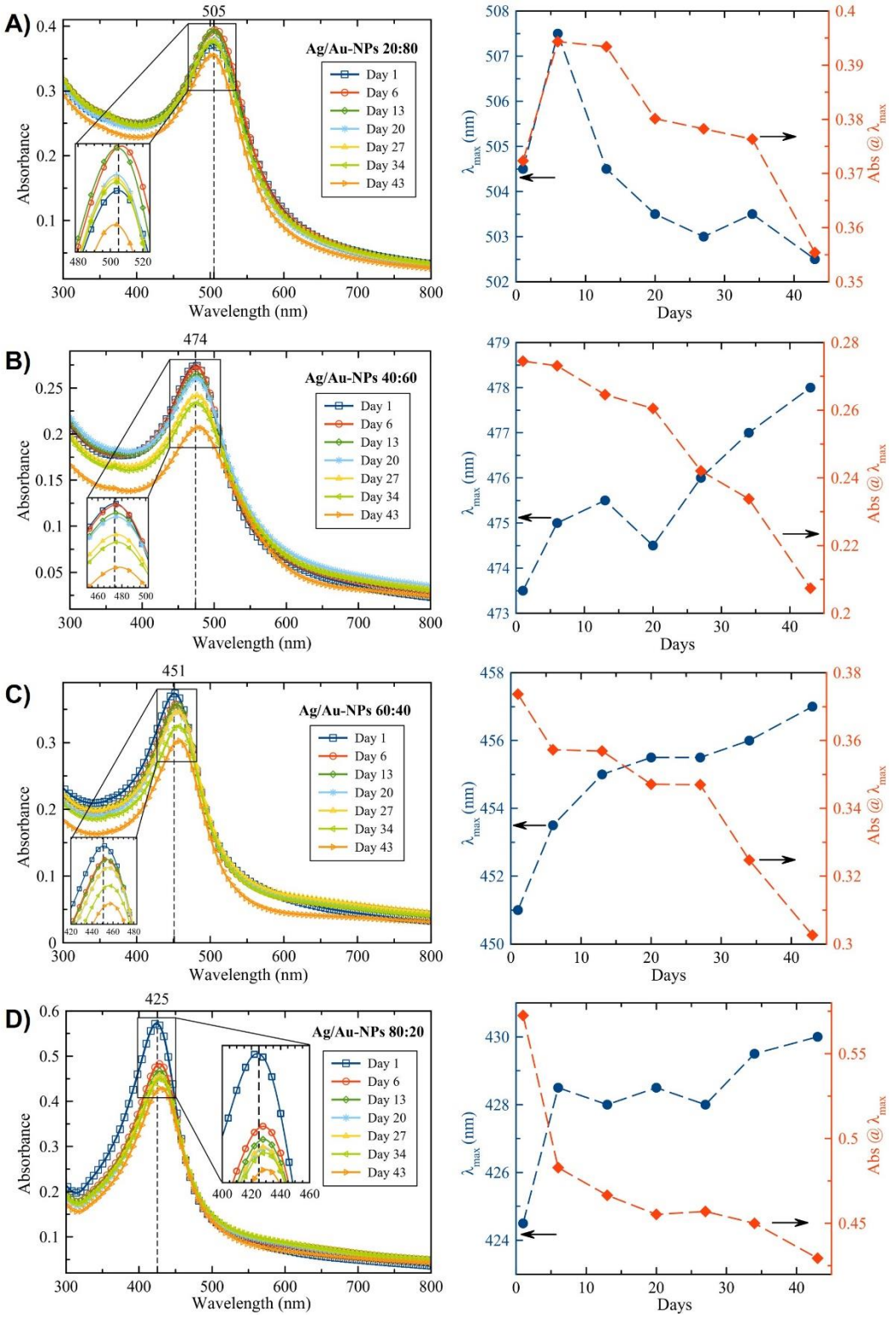


**Figure S2.** Study of the stability over the time of Ag/Au-NPs. Absorption spectra (left panels) and shift of $\lambda_{max}$ and absorbance at the given $\lambda_{max}$ as a function of time (right panels) for colloidal Ag/Au-NPs with Ag:Au ratio of **A**) 20:80, **B**) 40:60, **C**) 60:40, **D**) 80:20.

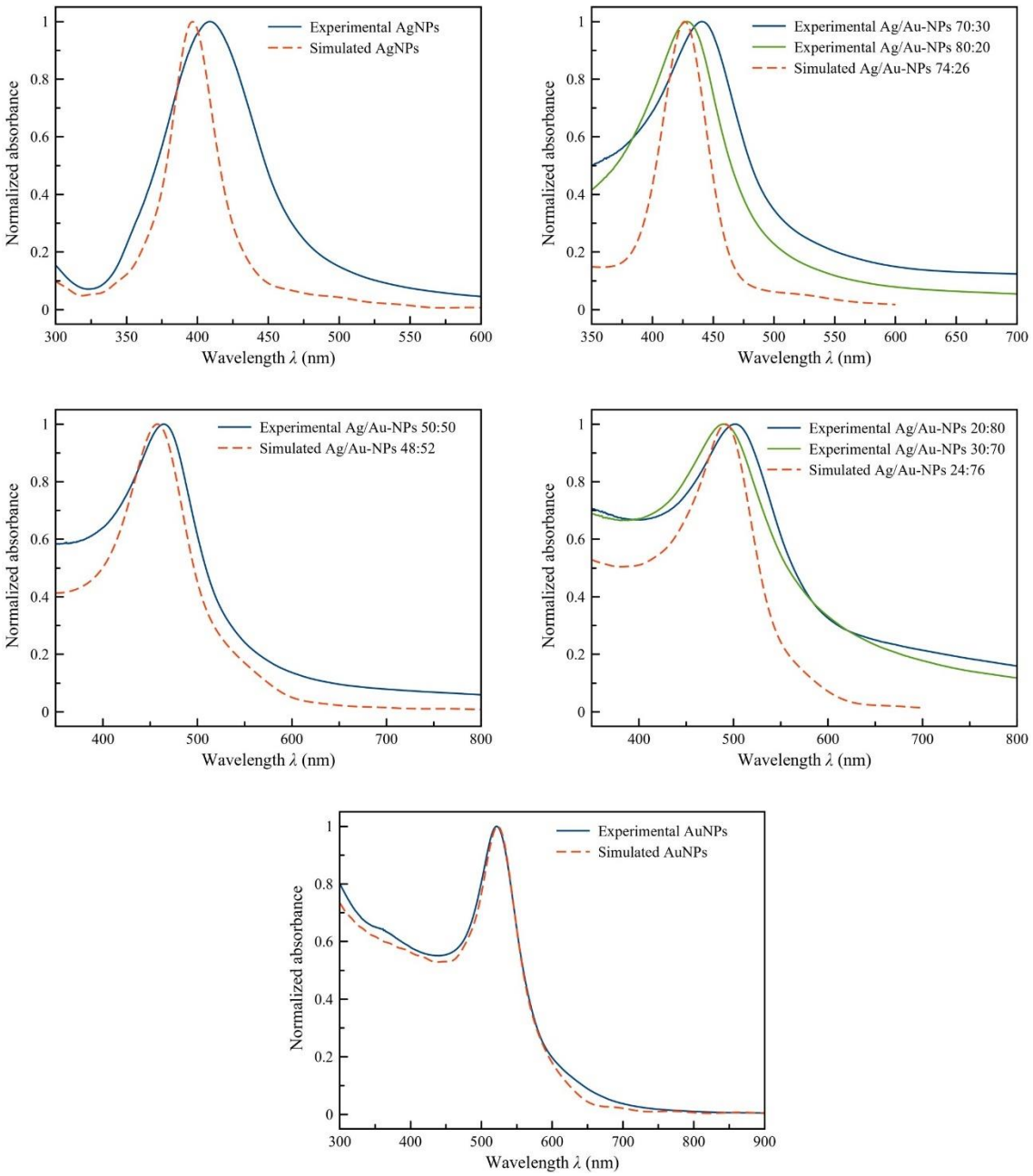


**Figure S3.** Comparisons between simulated and experimental absorption spectra for Ag/Au-NPs with different chemical compositions. The simulated spectra were calculated using 3D FDTD analysis.

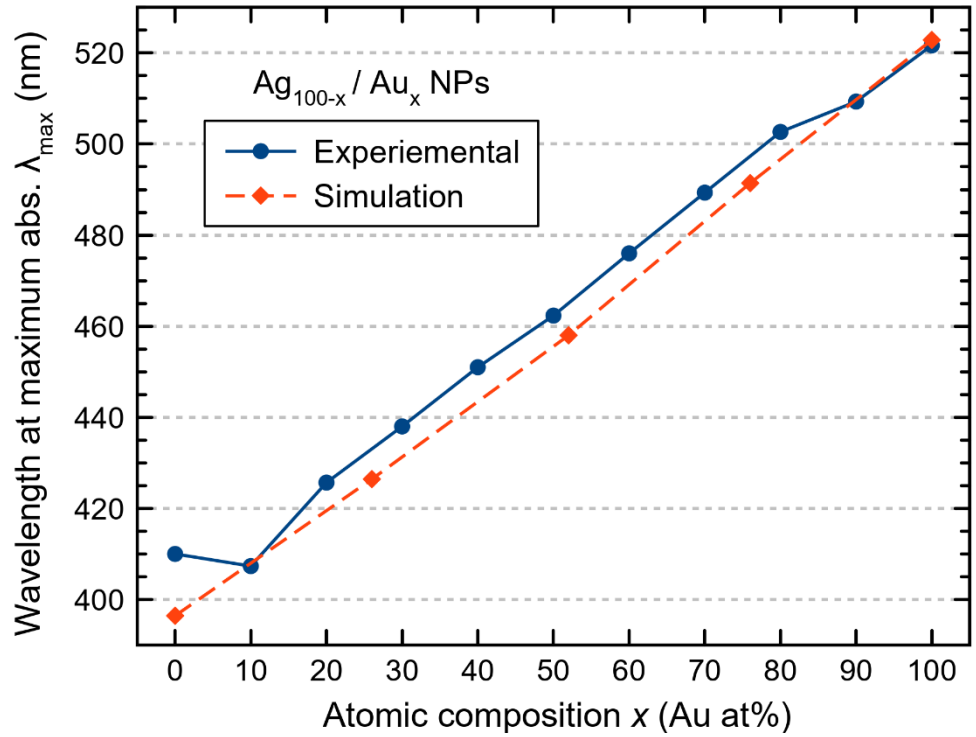


**Figure S4.** Comparison between the LSPR band positions obtained in the 3D FDTD simulations and the experimental values.

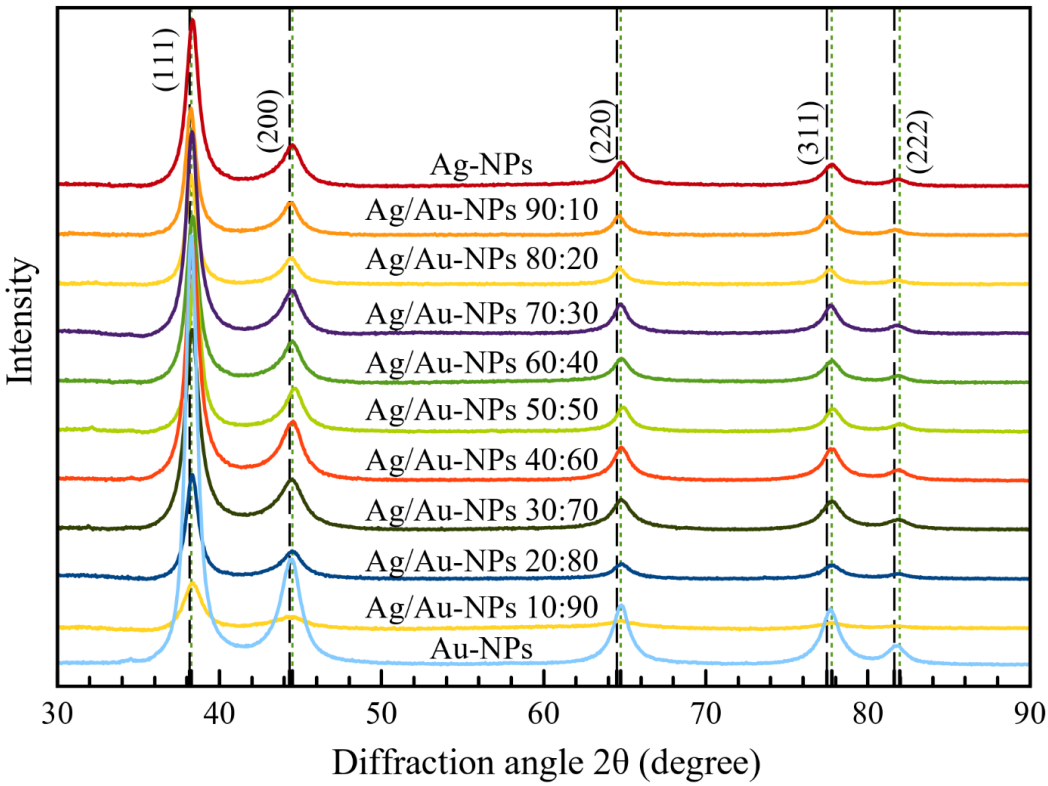


**Figure S5.** XRD spectra of the Ag/Au-NPs with different chemical compositions. Discontinuous and dotted lines correspond to expected diffraction peaks for FCC Ag and Au[1], respectively.

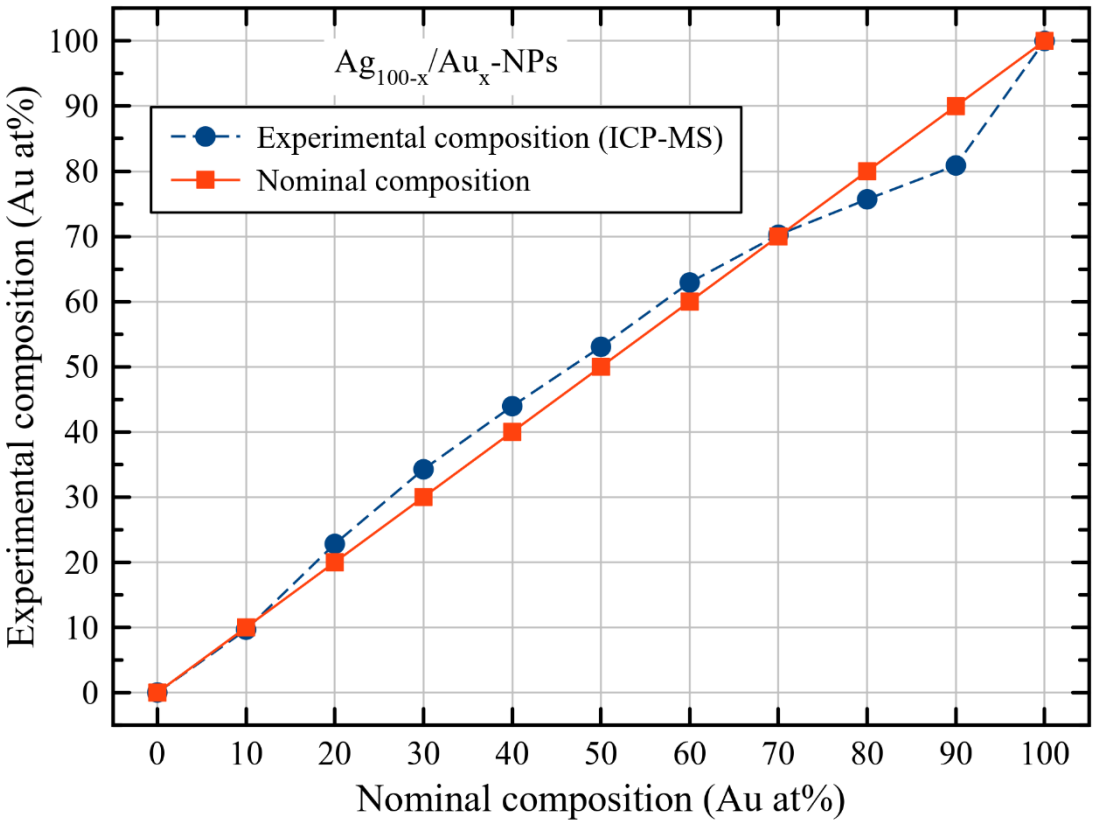


**Figure S6.** Experimental chemical composition (blue dots) of the Ag/Au-NPs found by ICP-MS as a function of nominal composition. The red squares correspond to the nominal composition of each sample. The blue dashed and red lines are guides for the eye.

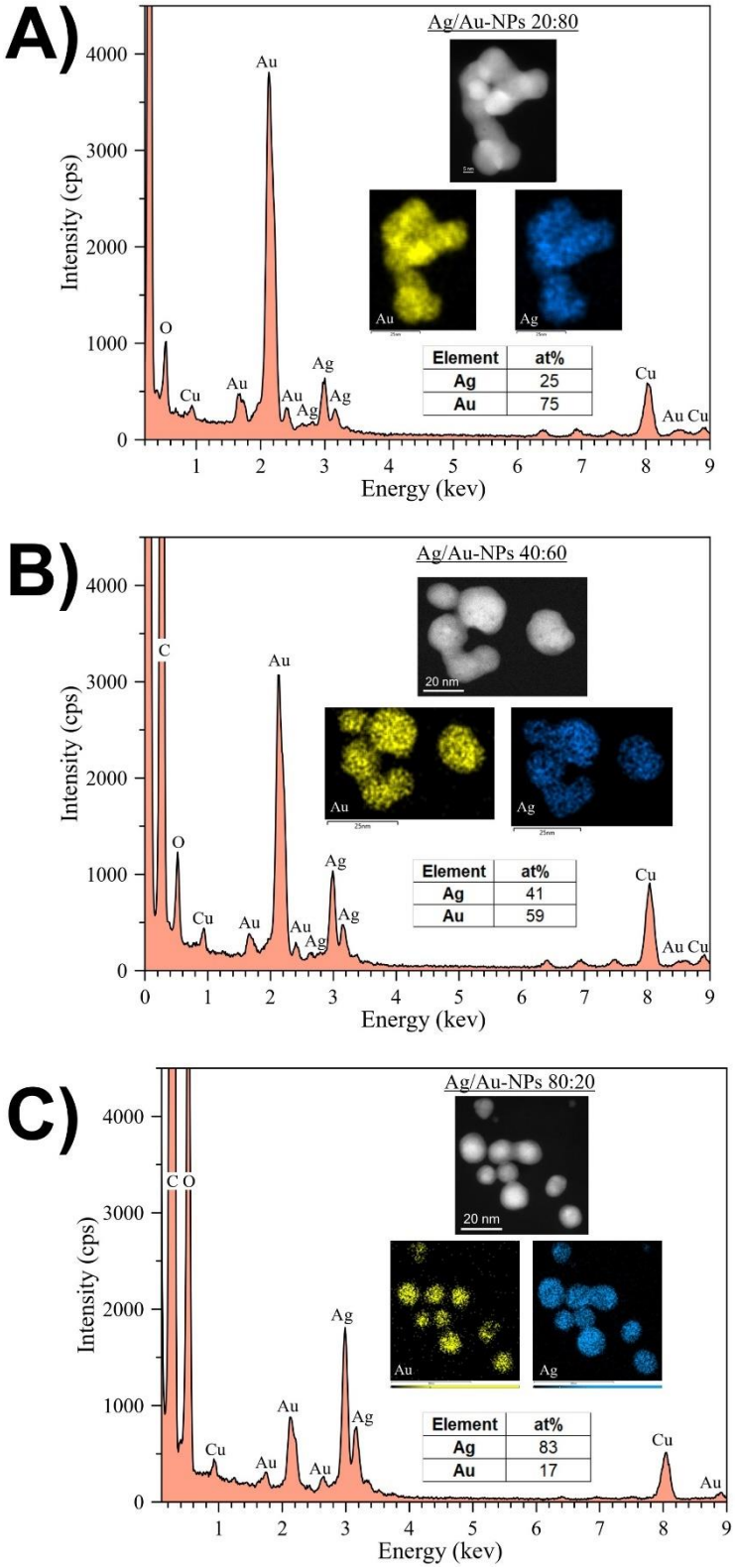


**Figure S7.** EDX spectra of Ag/Au-NPs with Ag:Au ratio of **A**) 20:80; **B**) 40:60; and **C**) 80:20.

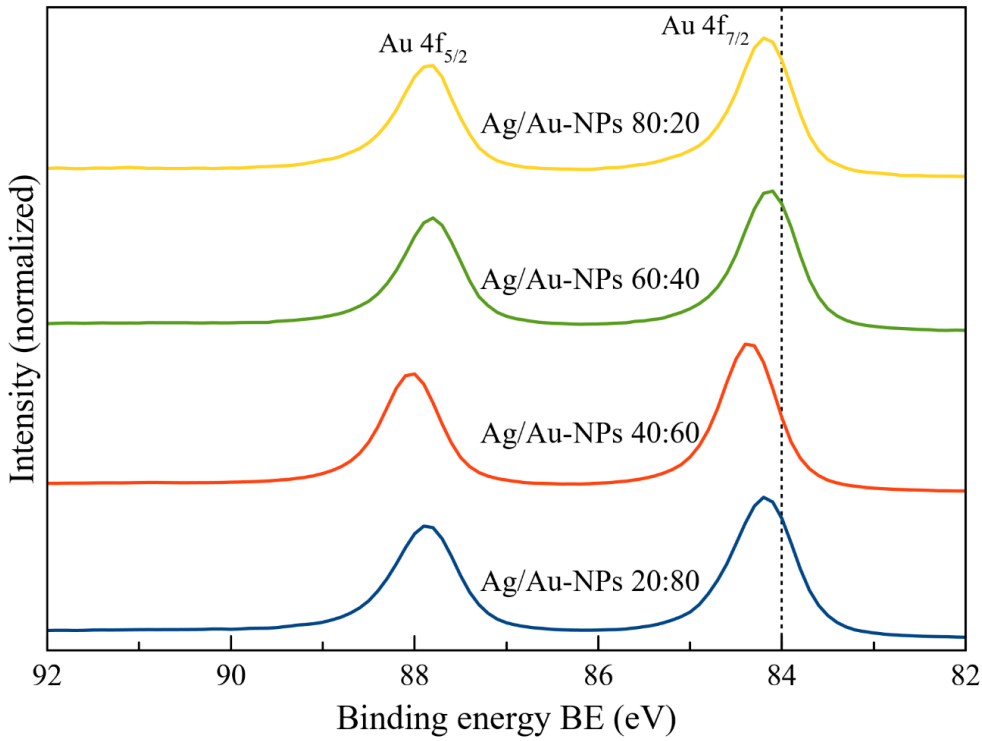


**Figure S8.** Au 4f core level peak for Ag/Au-NPs with Ag:Au ratio of 20:80, 40:60, 60:40 and 80:20. The dotted line correspond to the BE of Au $4f_{7/2}$ (84.0 eV) found in bulk Au[2].

**Table S1.** Experimental conditions for the synthesis of Ag/Au-NP colloids. In all samples, 500 µL of starch 1% (w/v) solution was used.

| Atomic Ratio (Ag:Au) | $AgNO_3$ 25 mM Solution (µL) | $NaAuCl_4$ 25 mM Solution (µL) |
|---|---|---|
| 100:0 | 250 | 0 |
| 90:10 | 450 | 50 |
| 80:20 | 400 | 100 |
| 70:30 | 350 | 150 |
| 60:40 | 300 | 200 |
| 50:50 | 250 | 250 |
| 40:60 | 200 | 300 |
| 30:70 | 150 | 350 |
| 20:80 | 100 | 400 |
| 10:90 | 50 | 450 |
| 0:100 | 0 | 250 |

**Table S2.** Crystallite size (*L*) Ag/Au-NPs extracted from XRD analysis (Figure S5).

| Ag/Au-NP Sample | Crystallite Size (*L*, in nm) |
|---|---|
| 100:0 | 15.3 ± 2.6 |
| 90:10 | 12.9 ± 3.9 |
| 80:20 | 13.1 ± 2.1 |
| 70:30 | 11.4 ± 1.7 |
| 60:40 | 9.6 ± 2.7 |
| 50:50 | 10.6 ± 2 |
| 40:60 | 8.7 ± 1.7 |
| 30:70 | 6.7 ± 1.3 |
| 20:80 | 8.3 ± 1.1 |
| 10:90 | 7.6 ± 2.8 |
| 0:100 | 11.2 ± 3.8 |

**Table S3.** Shift of the binding energy (ΔBE) for Ag $3d_{5/2}$ and Au $4f_{7/2}$ with respect to the bulk values (368.1 and 84.0 eV, respectively) of selected Ag/Au-NP samples obtained from the Ag 3d (Figure 7B) and Au 4f (Figure S8) core level peaks.

| Ag/Au-NP Sample | Ag $3d_{5/2}$ Shift (eV) | Au $4f_{7/2}$ Shift (eV) |
|---|---|---|
| 20:80 | 0.1 | 0.18 |
| 40:60 | 0.28 | 0.36 |
| 60:40 | 0.31 | 0.33 |
| 80:20 | 0.41 | 0.38 |

**Table S4.** Chemical composition of selected Ag/Au-NP samples extracted from the Ag3d (Figure 7B) and Au4f (Figure S8) core level peaks for Ag and Au, respectively.

| Ag/Au-NP Sample | Expected Atomic Ratio Ag:Au | Experimental Atomic Ratio Ag:Au |
|---|---|---|
| 20:80 | 0.25 | 0.27 |
| 40:60 | 0.67 | 0.65 |
| 60:40 | 1.50 | 1.52 |
| 80:20 | 4.00 | 3.80 |